COMPUTATIONAL METHODS IN APPLIED MATHEMATICS, Vol. 9 (2009), No. 3, pp. 309–318

IMAGE EDGE RESPECTING DENOISING WITH EDGE DENOISING BY A DESIGNER NONISOTROPIC STRUCTURE TENSOR METHOD

N. SANTITISSADEEKORN[1] AND E. M. BOLLT[2]

Abstract — We consider image denoising as the problem of removing spurious oscillations due to noise while preserving edges in the images. We will suggest here how to directly make infinitesimal adjustment to standard variational methods of image denoising, to enhance desirable target assumption of the noiseless image. The standard regularization method is used to define a suitable energy functional to penalize the data fidelity and the smoothness of the solution. This energy functional is tailored so that the region with small gradient is isotropically smoothed whereas in a neighborhood of an edge presented by a large gradient smoothing is allowed only along the edge contour. The regularized solution that arises in this fashion is then the solution of a variational principle.

To this end the associated Euler — Lagrange equation needs to be solved numerically and the half-quadratic minimization is generally used to linearize the equation and to derive an iterative scheme. We describe here a method to modify Euler — Largrange equation from commonly used energy functionals, in a way to enhance certain desirable preconceived assumptions of the image, such as edge preservation. From an algorithmic point of view, we may deem this algorithm as a smoothing by a local average with an adaptive gradient-based weight. However, this algorithm may result in noisy edges although the edge is preserved and noise is suppressed in the low-gradient regions of the image. The main focus here is to present an edge-preserving regularization in the aforementioned view point, and to provide an alternative and simple way to modify the existing algorithm to mitigate the phenomena of noisy edges without explicitly defining step where we specify an energy functional to be minimized.

2000 Mathematics Subject Classification: 68U10.

Keywords: denoising, regularization, edge-preserving.

1. Introduction

Reconstructing an image contaminated by noise is a very important task in image processing. During recent years, several approaches have been developed for image reconstruction along three main categories: (1) wavelet-based methods introduced by Donoho and Johnstone [6, 7], (2) stochastic or statistical methods such as Markov random fields (MRF's) pioneered by Geman and Geman [8], and (3) variational approaches [2–4, 9, 11, 13] with

[1] *School of Mathematics and Statistics, University of New South Wales*, Sydney, NSW 2052, Australia. E-mail: santin@clarkson.edu

[2] *Department of Mathematics and Computer Science, Clarkson University*, Potsdam, NY 13699-5815, USA. E-mail: bolltem@clarkson.edu

partial differential equations (PDE's) [1, 10]. The variational approach minimizes a suitable energy functional to smooth only the homogeneous regions surrounded by sharp edges without degrading the slope of the edges. We first review the deterministic edge-preserving variational approach introduced in [2, 4, 13] that employs the half-quadratic minimization to construct an algorithm. However, we view this algorithm as an iterative scheme with an adaptive gradient-based weight for a local average, which may also be described as nonlinear diffusions [1, 10]. Note also that several recent works have been developed based on the coherent structure analysis using the gradient structure tensor to determine the location and orientation of the edges [12, 14]. Then, we empirically demonstrate a result to show that although the edges are preserved, the regions near the edges are still noisy as much as they are in the noised initial image. Thus, we present a modification of the iterative algorithm to allow the smoothing along the edge to eliminate the oscillations near the edges and demonstrate experimental results on synthetic and real images.

2. Review: edge-preserving regularization

First we review the now traditional approach [2, 4] as the counterpoint as contrast to our method to come. A noisy image $f(x)$ can be restored by a minimization of the following energy functional:

$$F(u) = \int_\Omega |f(x) - u(x)|^2 \, dx + \lambda \int_\Omega \phi(\nabla |u(x)|^2) \, dx, \tag{2.1}$$

where $x \in \Omega$ and Ω is an open bounded set in $\mathbb{R}^2$. Throughout this paper, we will denote the reconstructed image by $u(x)$ and the noisy image by $f(x)$. The first integral term is responsible for the data fidelity and the second is the smoothing term with a parameter λ as a positive weight constant. The function ϕ is chosen to allow smoothing within texture regions and prevent smoothing across the edge. The criterions of the function ϕ can be found in [2, 4, 13]. In general, the functional Eq. (2.1) is not convex and its associated Euler — Lagrange equation is nonlinear. However, the half-quadratic regularization can be used to recast Eq. (2.1) as follows

$$J(u, b) = \int_\Omega |f(x) - u(x)|^2 \, dx + \lambda \int_\Omega (b(\nabla |u(x)|^2) + \psi(b)) \, dx, \tag{2.2}$$

where b is an auxiliary function usually called the dual variable and the convex function

$$\psi(b) = \theta((\theta')^{-1}(b)) - b(\psi')^{-1}(b) \quad \text{and} \quad \theta(s) = \phi(\sqrt{s}). \tag{2.3}$$

The new energy functional Eq. (2.2) is not convex with respect to the pair (u, b) but it is convex in u when b is fixed and vice versa. Therefore, for each fixed b we have a convex functional and the minimization is linear. Conversely, for each fixed u the unique minimum of Eq. (2.2) is obtained at

$$b_{\inf}(u) = \frac{\phi'(\nabla |u(x)|)}{2|u(x)|}. \tag{2.4}$$

This leads to the following algorithm.

Algorithm 2.1.

1. Initialize (u^0, b^0)

2. Repeat

   (a) Solve the associated Euler — Lagrange equation of $u = \inf_u J(u, b^n)$, that is,

$$(u^{n+1} - f) - \lambda \operatorname{div}(b^n \nabla u^{n+1}) = 0 \quad \text{in} \quad \Omega \tag{2.5}$$

   (b) Solve $b = \inf_b J(u^{n+1}, b)$. This can be obtained at

$$b^{n+1} = \frac{\phi'(\nabla|u|)}{2|u|} \tag{2.6}$$

3. Repeat until convergence

We refer the convergence analysis of this fixed point iteration to Dobson and Vogel [5].

Now observe that the auxiliary variable b can be considered as a weight function to the anisotropic smoothing on u by the operator $\mathtt{div}(b\nabla u)$. Remark that if $b \equiv 1$, we have an isotropic smoothing by the Laplace operator that is known to blur the edges. Since the variable b tends to zero at the edges with a large $|\nabla u|$, we have that near the edges the solution u is kept close to the observed image $f(x)$, and hence the edge is preserved as much as it is in the original image $f(x)$. For this reason, the overshoot and oscillation near the edges due to noise still appear in the solution u. Although one may argue that this help to increase the contrast of the edges, we consider it undesirable because it can cause instability in the above iterative algorithm when noise is large and it may bring out an incorrect contrast to the entire image. We would also like to point out that the image restored by minimizing Eq. 2.2 agrees very well with the isotropically smoothed image by the Laplacian operator at the low-gradient regions surrounded by the edges since we have $b \approx 1$ in these regions. Another limitation of the above method is that the variable b interpreted as an edge detector can be noisy. These two limitations are demonstrated by the example illustrated in Figure 2.1 and Figure 2.2, where the fixed point iteration is used to solve the the Euler — Lagrange equation and the function ϕ is chosen as

$$\frac{\phi'(s)}{2s} = \frac{1}{\sqrt{1+s^2}}. \tag{2.7}$$

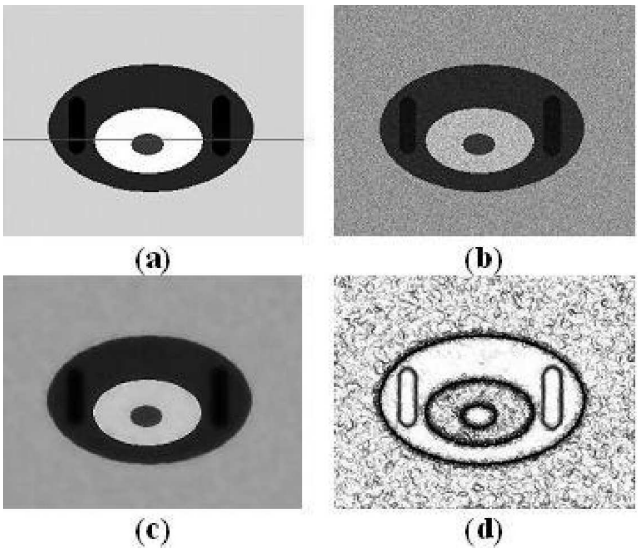

Fig. 2.1. (a) A true image $f_0(x)$ of the size of 295×230 pixels. The red horizontal line shows the location of the 1-d slice shown in Figure 2.2. (b) A noisy image (SNR$\approx$ 13.4). (c) A restored image by the edge-preserving regularization with the smoothing parameter $\lambda = 10$, (d) The edge variable b

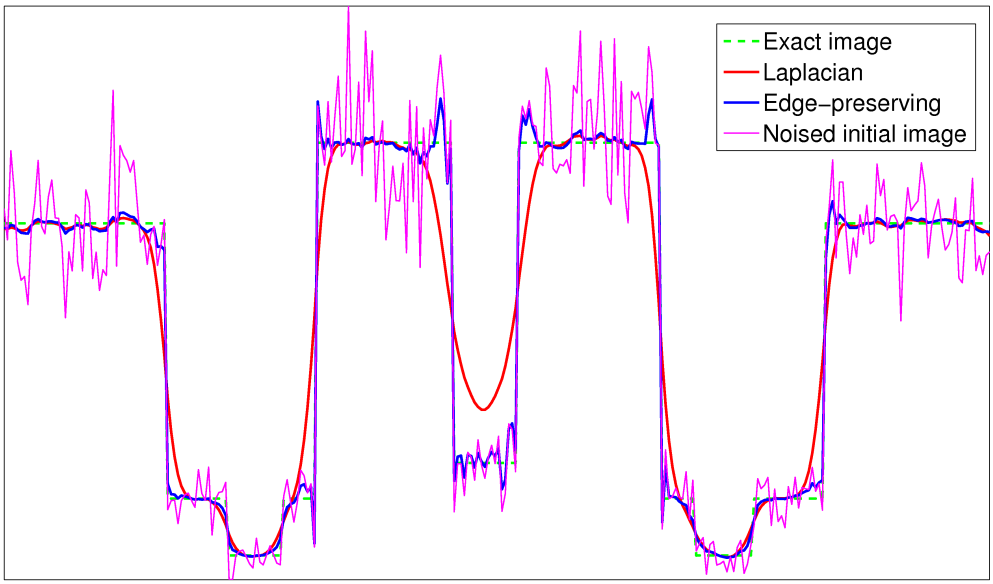

Fig. 2.2. The 1-d slice at the location of the red line shown in Figure 2.1. Clearly, the edges of the image reconstructed by the edge-preserving regularization is preserved as desired but they are noisy, especially at the large edge. Notice that the images denoised by the Laplacian operator and the edge-preserving scheme coincide at the low-gradient regions, which include the small-scale edges

3. Modified algorithm by designer tensor

As explain in the previous section we may view the edge-preserving regularization as an iterative scheme that iteratively smooth edges by using the variable b as an adaptive weight for smoothing on u. However, the oscillations at edges may retain in the image and the auxiliary variable deemed as the edge detector can be very noisy. First, let us present an approach used also in [13] to suppress the small spurious oscillations due to noise for the edge variable b and specify a sensitivity threshold to keep only edges with edge strength above the threshold. For a given threshold τ_0, where $\tau_0 \in (0,1)$ we define the function $\tilde{\phi}$ as

$$\tilde{\phi}(s) = \frac{1}{\sqrt{1+(s/\kappa)^2}}, \tag{3.1}$$

where

$$\kappa = \left(\frac{\tau_0^2}{1-\tau_0^2}\right)^{1/2}. \tag{3.2}$$

Figure 3.1 illustrates the role of the threshold τ_0. We can see that as τ_0 tends to 1 the small oscillations due to noise are eliminated. However, if τ_0 is "too" close to 1, as a consequence, the edge with a low contrast are also suppressed.

Now, we suggest a direct modification to the iterative algorithm of the edge-preserving regularization to reduce the overshoot and oscillation at the edges as follow

Algorithm 3.1 (designer diffusion tensor)

1. Initialize (u^0, b^0). Set the threshold τ_0 and κ as in Eq. (3.2) and set the positive weight parameters λ and α

   (a) Solve the equation

   $$(u^{n+1} - f) - \lambda \operatorname{div}(b^n \nabla u^{n+1}) - \alpha \operatorname{div}((1 - b^n)\nabla f) = 0 \quad \text{in} \quad \Omega \tag{3.3}$$

   (b) Update the edge variable $b : b^{n+1} = \tilde{\phi}(\nabla |u|)$

   (c) Normalize the edge variable b so that b varies from 0 to 1

2. Repeat until convergence

In comparison to the previous algorithm, we have introduced the following difference. Here we have merely added to Eq. (2.5) an additional term of the form

$$\alpha \operatorname{div}((1 - b^n)\nabla f) \tag{3.4}$$

to smooth along the edges. The idea is to use the weight $1 - b$, which approximates the edge contour, for an anisotropic diffusion on the noised initial image. *Therefore, this modified algorithm prevents an overshoot and oscillation at the edge.* Figure 3.2 shows a denoising example of the same 1-d slice in Figure 2.2 restored by our suggested algorithm. We can see that the overshoots at the edges are significantly reduced while the edges is still preserved. Figure 3.3 shows an example of a noisy edge due to the overshooting problem in comparison with the smooth edge obtained from our algorithm. To justify the influence of α to the numerical performance, we use the following norm, denoted by E, to measure an error:

$$E(u) = \frac{\|u - f_0\|}{\|f_0\|} + \left\| \frac{|\nabla u|}{\||\nabla u|\|} - \frac{|\nabla f_0|}{\||\nabla f_0|\|} \right\|, \tag{3.5}$$

where f_0 is the true, noiseless image, $\nabla f = (\partial f/\partial x, \partial f/\partial y)$, and $\|\cdot\|$ denotes the 2-norm. The first term in the above norm measures an error in term of data fidelity and the second term measures the error in"steepness" of the edges. Figure 3.4(a) shows quantitative tests of the parameter α based on the above error norm for different values of λ. Furthermore, one may observe that the performance in term of λ, based on the above error norm, becomes "saturate" as λ increases and this saturation can also be observed from the SNR plot as shown in Figure 3.5.

Now we apply our proposed algorithm to the noisy image of Lena (512×512 pixels). Figure 3.6 compare the results using the conventional edge-preserving regularization and the modified algorithm. We can see that the edge and other discontinuities are preserved and noise is suppressed in both methods. However, after a careful observation as illustrated in Figure 3.7 we can clearly see the noisy edges of the image denoised by the edge-preserving regularization whereas these noisy edges are smoothed along the edge by our modified algorithm. Figure 3.4(b) shows the error given by 3.5 for different values of λ. Notice that the error reaches the optimal at a larger value of α since the size of the Lena image is twice as large as that of the previous one, whence makes the norm of the data fidelity term in the cost function 2.1 larger. Thus, this requires, for a given λ, a larger value of parameter α so that the error reaches the optimal.

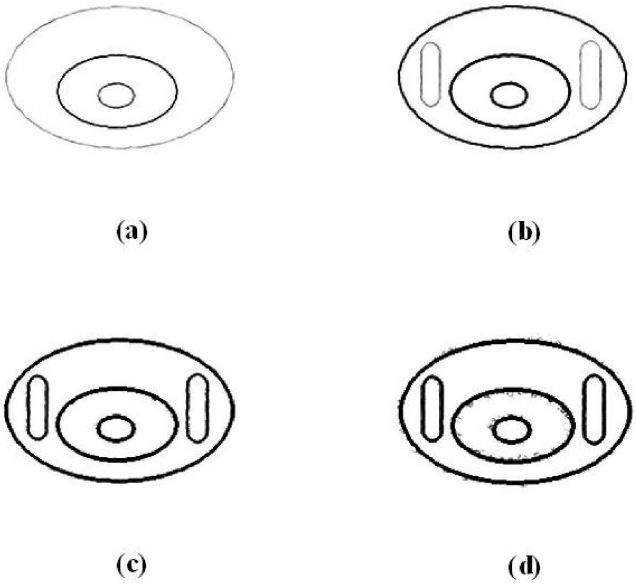

Fig. 3.1. Illustration of the behavior of the sensitivity threshold τ_0 on the edge variable b, which varies from 0 to 1. From (a) to (d), τ_0 varies from 0.99, 0.9, 0.85 and 0.8, respectively. This shows that as the threshold tends to one the edge with a low contrast will be ignored. However, a low value of τ_0 may allow a presence of small oscillations due to noise in the edge variable b

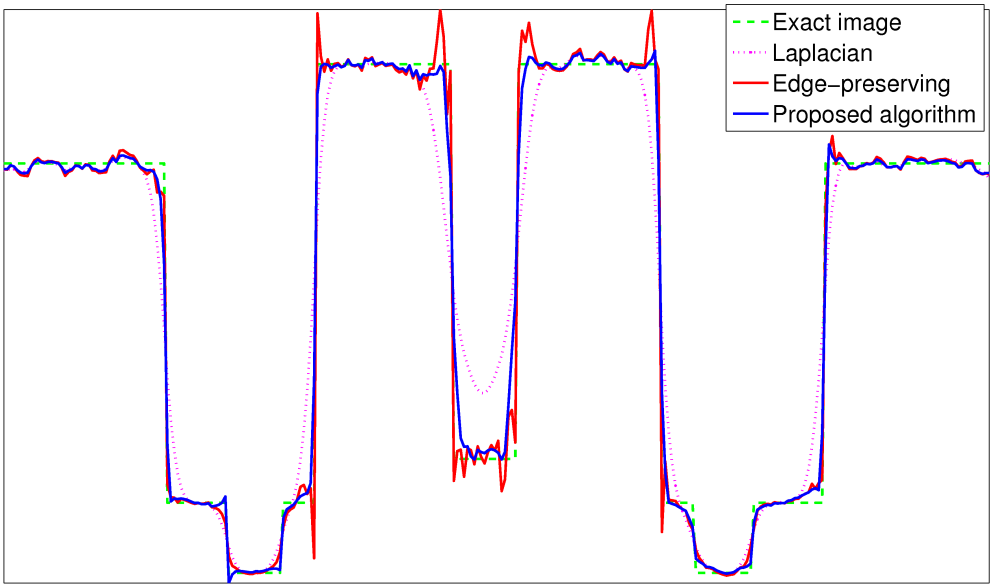

Fig. 3.2. Illustration of the restored image by the suggested algorithm with the same $\lambda = 10$, as used to obtain the result in Figure 2.2, and $\alpha = 2$. In comparison with the image restored by the edge-preserving regularization, the oscillations at the large edges are moderated while the edges are not over-smoothed

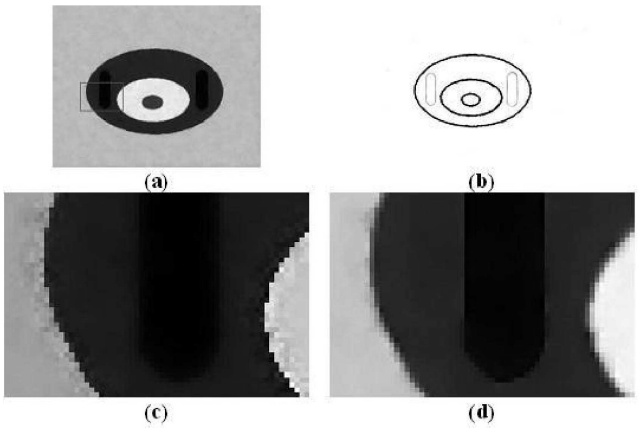

F i g. 3.3. (a) The restored image by the proposed algorithm. (b) The edge variable obtained from the proposed algorithm. (c) The enlarged picture of the region surrounded by the square in (a) from the image restored by the edge-preserving regularization (d) The enlarged picture of the same region of the image restored by the suggested algorithm, which shows a smoother edge since the oscillations at the edges are mitigated

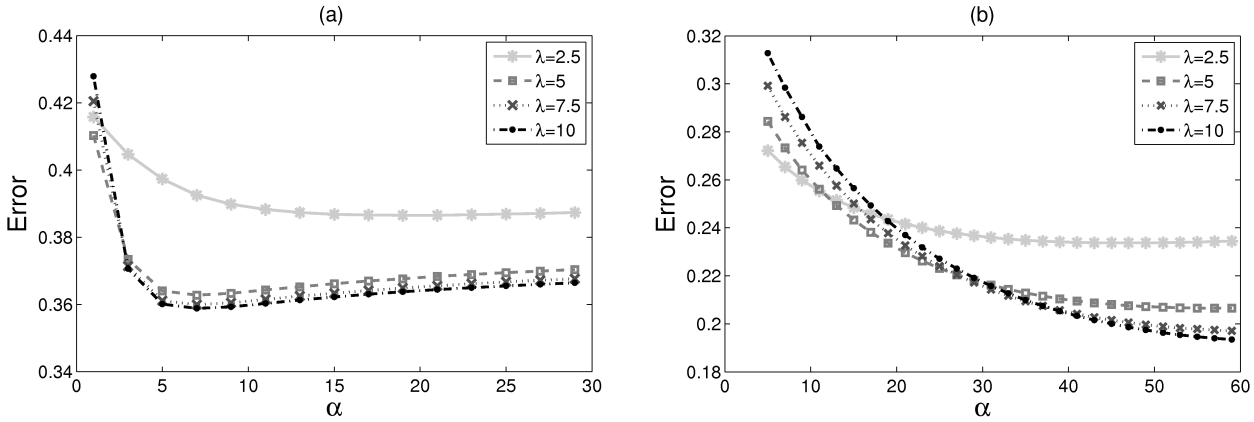

F i g. 3.4. The influence of the parameter α on the error given by (3.5). (a) The error as a function of α for the image shown in Fig. 2.1(a). After being optimal, the error slightly increases. (b) The error for the Lena image. The error reaches the optimal at a comparatively larger value of α. This is due to the size of the Lena image is approximately twice as large

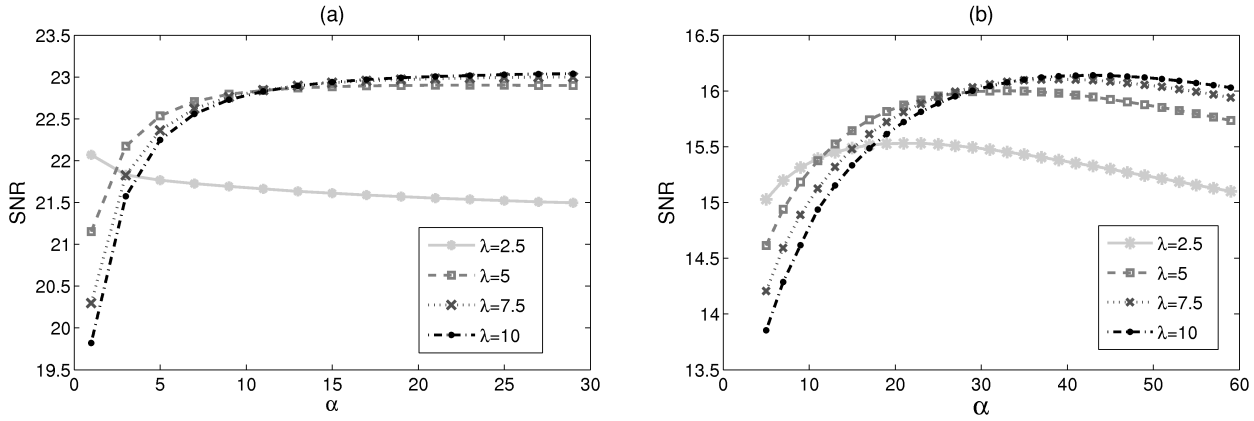

F i g. 3.5. The influence of the parameter α on the SNR. (a) The SNR as a function of α for the image shown in Fig. 2.1(a). Again, after being optimal, the SNR slightly decreases. (b) The SNR for the case of the Lena image

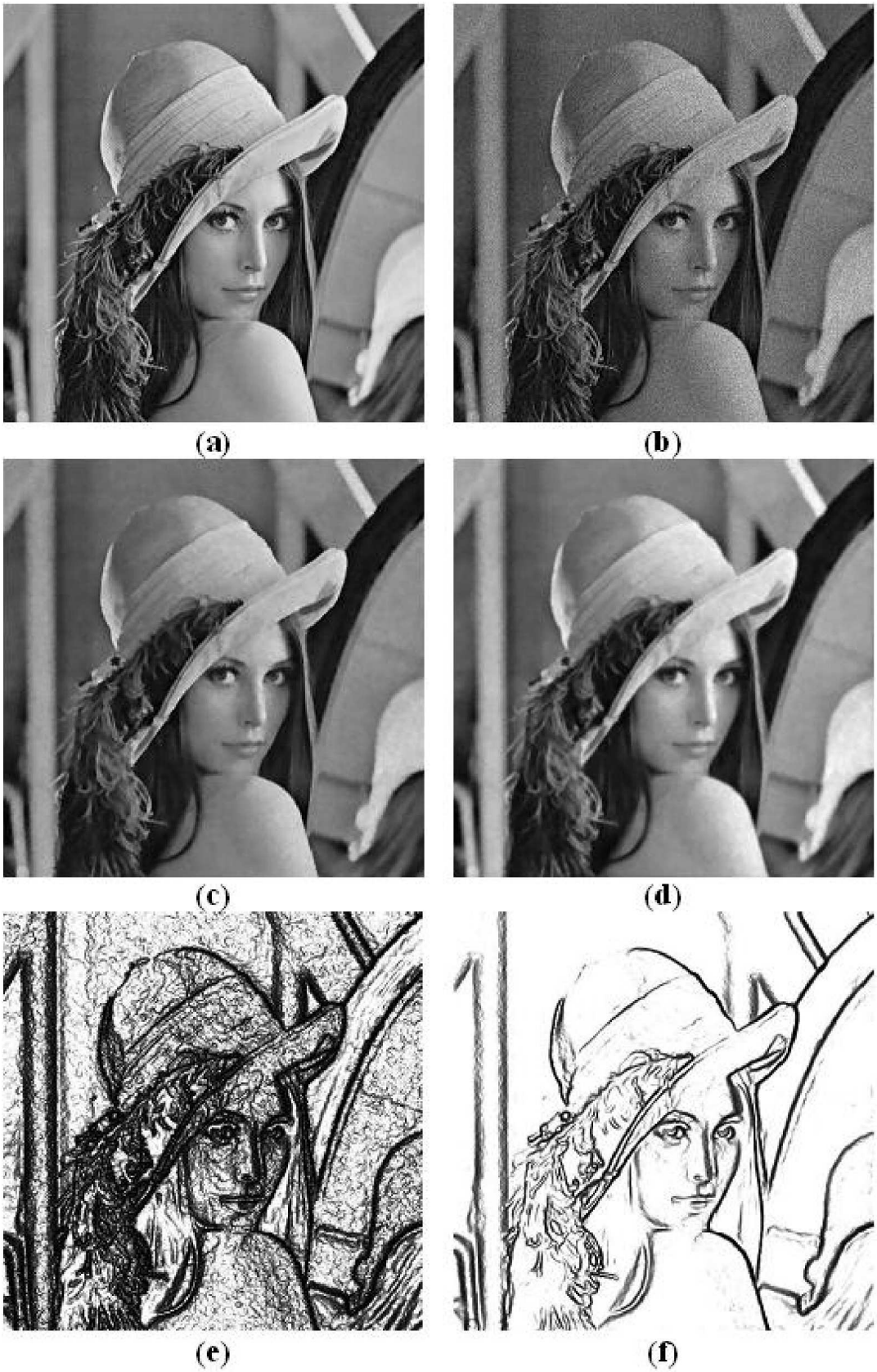

Fig. 3.6. (a) The true image of Lena (512×512 pixels). (b) The Lena image corrupted with zero-mean Gaussian noise(SNR$\approx$ 5.8). (c) and (e) The image and edge variable obtained from the edge-preserving regularization. (d) and (f) The image and edge variable reconstructed using the proposed algorithm

Fig. 3.7. We enlarge a part of Lena to closely observe and compare the result using (a) the edge-preserving regularization and (b) our proposed algorithm. Notice that the noisy edges appear in (a) but they are smooth in (b)

4. Summary

The edge-preserving regularization method is used to remove small oscillations due to noise while preserving the edges in an image. We view this method as an iterative scheme with an adaptive gradient-based weight for a local average. The result of this method not only provide a denoised image with sharp edges but also has a potential use as an edge detector. However, our empirical result demonstrates that this method results in noisy edges in the denoised image and the unacceptable noisy edge variable if we want to use it as an edge detector as well. Moreover, the overshooting at the edge occur as a generic problem of this algorithm. We then improve this method at the level of the iterative scheme by adding a term to allow a smoothing along the edge contour so that the overshooting near the edges and the noisy background in the edge variable is diminished.

References

1. L. Alvarez, P. L. Lions, J. M. Morel, and T. Coll, *Image selective smooothing and edge detection by nonlinear diffusion ii*, SIAM J. Numer. Anal., **29** (1992), pp. 845–866.

2. G. Aubert and P. Kornprobst, *Mathematical Problems in Image Processing: Partial differential Equations and the Calculus of Variations*, Springer-Verlag, New York, 2002.

3. A. Blake and A. Zisserman, *Visual Reconstruction*, MIT Press, Cambridge, MA, 1987.

4. P. Charbonnier, L. Blanc-Féraud, G. Aubert, and M. Barlaud, *Deterministic edge-preserving regularization in computed imaging*, IEEE Transaction of Image Processing, **6** (1997), no. 2, pp. 298–311.

5. D. C. Dobson and C. R. Vogel, *Convergence of an iterative method for total variation denoising*, SIAM Journal on Numerical Analysis, **34** (1997), no. 5, pp. 1779–1791.

6. D. L. Donoho, *De-noising by soft-thresholding*, IEEE Trans. Inform. Theory, **41** (1995), no. 3, pp. 613–627.

7. D. L. Donoho and I. M. Johnstone, *Ideal spatial adaptation by wavelet shrinkage*, Biometrika, (1994), no. 81, pp. 425–455.

8. S. Geman and D. Geman, *Stochastic relaxation, gibbs distribution, and the bayesian restoration of images*, IEEE Trans. Pattern Anal. MAch. Intell., **6** (1983), pp. 721–741.

9. D. Mumford and J. Shah, *Optimal approximations by piecewise smooth functions and associated variational problems*, Commun. Pure Appl. Math., **42** (1989), pp. 557–685.

10. P. Perona and J. Malik, *Scale-space and edge detection using anisotropic diffusion*, IEEE Trans. Pattern Anal. MAch. Intell., **12** (1990), pp. 629–639.

11. L. Rudin, S. Osher, and E. Fatemi, *Nonlinear total variation based on noise removal algorithm*, Physica D, **60** (1992), pp. 259–268.

12. H. Takeda, S. Farsiu, and P. Milanfar, *Kernel regression for image processing and reconstruction*, IEEE Transaction of Image Processing, **16** (2007), no. 2, pp. 349–366.

13. S. Teboul, L. Blanc-Féraud, G. Aubert, and M. Barlaud, *Varitational approach for edge-preserving regularization using coupled pde's*, IEEE Transaction of Image Processing, **7** (1998), no. 3, pp. 387–397.

14. H. Wang, Y. Chen, T. Fang, J. Tyan, and N. Ahuja, *Gradient adaptive image restoration and enhancement*, International Conference on Image Processing, 2006.